CHEMISTRY
A EUROPEAN JOURNAL

Anion Receptors Containing -NH Binding Sites: Hydrogen-Bond Formation or Neat Proton Transfer?

Valeria Amendola,[a] Massimo Boiocchi,[b] Luigi Fabbrizzi,*[a] and Arianna Palchetti[a]

Abstract: When the amide-containing receptor $\mathbf{1}^+$ is in a solution of dimethyl sulfoxide (DMSO) in the presence of basic anions (CH_3COO^-, F^-, $H_2PO_4^-$), it undergoes deprotonation of the -NH fragment to give the corresponding zwitterion, which can be isolated as a crystalline solid. In the presence of less basic anions (Cl^-, Br^-, NO_3^-), $\mathbf{1}^+$ establishes true hydrogen-bond interactions of decreasing intensity. The less acidic receptor $\mathbf{2}^+$ undergoes neat proton transfer with only the more basic anions CH_3COO^- and F^-, and establishes hydrogen-bond interactions with $H_2PO_4^-$. An empirical criterion for discerning neutralisation and hydrogen bonding, based on UV/Vis and ^{1}H NMR spectra, is proposed.

Keywords: anions · hydrogen bonds · molecular recognition · proton transfer · receptors

Introduction

Anions play an important role in medicine, biology, environmental and food sciences,[1] accounting for the increasing interest in the design of synthetic anion receptors. Methodologies for the prompt detection and quantitative determination of anions are being developed and, within the last decade, a variety of molecular sensors for anions have been synthesised.[2] Most of these sensors contain chromogenic or fluorogenic groups that are covalently or non-covalently linked to the receptor moiety, thus enabling the colorimetric and fluorimetric sensing of anions with both temporal and spatial resolution.[3] The nature of the anion–receptor interaction is a matter of choice for the designer; it can be electrostatic, in which case the receptor must be equipped with positively charged groups (e.g., ammonium, alkylammonium, pyridinium, guanidinium),[4] or it can be based on hydrogen bonding. In the latter case, the receptor must provide hydrogen-bond-donor groups, in most cases the -NH fragment of carboxyamides, sulfonamides, ureas, thioureas and pyrroles.[5] Receptors based on hydrogen bonding are expected to interact principally with anions containing the most electronegative atoms, fluoride and oxygen (in the form of inorganic and organic oxo anions), while recognition studies are preferably carried out in aprotic media (e.g., dimethyl sulfoxide (DMSO), MeCN, $CHCl_3$), to avoid competition of the solvent (e.g., water or alcohols) as a hydrogen-bond donor.

From this perspective, we considered the possibility of designing anion receptors that contained both a positively charged group and a hydrogen-bond-donor group. The reasons for this approach were two-fold: firstly, the presence of a proximate, positive charge should enhance the tendency of the -NH group to act as a hydrogen-bond donor, and secondly, the positively charged group itself should provide additional electrostatic interaction with the negatively charged analyte. We prepared the molecular ions $\mathbf{1}^+$ (1-benzyl-3-(toluene-4-sulfonylamino)pyridinium; -NH binding site from the *p*-toluenesulfonamide moiety, positive charge from the benzylpyridinium fragment), and $\mathbf{2}^+$ (2-benzyl-9*H*-β-carbolin-2-ium; -NH from the pyrrole subunit, positive charge again from a benzylpyridinium fragment).

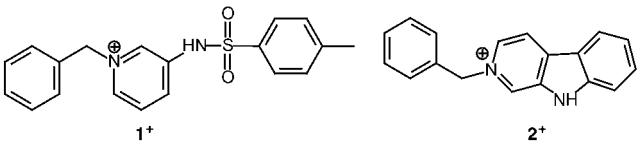

$\mathbf{1}^+$ $\mathbf{2}^+$

The interaction of $\mathbf{1}^+$ and $\mathbf{2}^+$ with a variety of anions was investigated by performing titration experiments in DMSO, and analysing the products by UV/Vis spectrophotometry

[a] Dr. V. Amendola, Prof. L. Fabbrizzi, A. Palchetti
Dipartimento di Chimica Generale, Università di Pavia
viale Taramelli 12, 27100 Pavia (Italy)
Fax: (+39) 0382-528-544
E-mail: luigi.fabbrizzi@unipv.it

[b] Dr. M. Boiocchi
Centro Grandi Strumenti, Università di Pavia
via Bassi 21, 27100 Pavia (Italy)

DOI: 10.1002/chem.200400592

and ^{1}H NMR spectroscopy. We demonstrated that anion–receptor interactions may involve either a neat proton transfer or hydrogen-bond interactions, depending on the intrinsic acidity of the -NH group and the basic tendencies of the anion.

Results and Discussion

Both $\mathbf{1}^+$ and $\mathbf{2}^+$ were obtained as hexafluorophosphate salts, following reaction of the parent molecules with benzylbromide and subsequent recrystallisation in the presence of $[NH_4]PF_6$. The crystalline form of **1**-PF_6 was isolated and its molecular structure was determined by X-ray diffraction studies (Figure 1). The structure reveals the reciprocal inter-

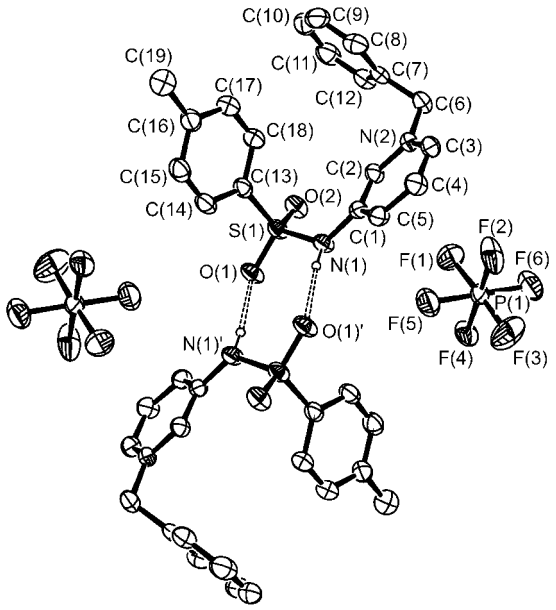

Figure 1. The ORTEP view of the **1**-PF_6 molecule shows that two symmetrically equivalent $\mathbf{1}^+$ ions (related by an inversion centre) are linked by hydrogen bonds (dashed lines) to form a molecular dimer (thermal ellipsoids are drawn at the 30% probability level, hydrogens bonded to carbon atoms were omitted for clarity). Features of the N–H···O interaction are N(1)···O(1)′ = 2.938(3) Å, H(1N)···O(1)′ = 2.074(24) Å, N(1)–H(1N)···O(1)′ = 172.8(23)° (symmetry code ′ = $-x$, $-y+1$, $-z$).

action of two $\mathbf{1}^+$ ions, by means of hydrogen bonds involving the -NH group from one ion and a sulfonamide oxygen atom from the other. Each $\mathbf{1}^+$ ion exhibits a conformation that may minimise the intermolecular steric repulsions within the hydrogen-bonded dimer. In any case, interactions do not involve the PF_6^- ion, which was deliberately chosen to act as a very poor hydrogen-bond acceptor.

Next, a solution of **1**-PF_6 in DMSO was titrated with a solution of a $[Bu_4N]X$ salt in DMSO, in which X^- represented the F^-, CH_3COO^-, $H_2PO_4^-$, NO_3^-, Cl^- or Br^- ion. In all cases, the resulting solution had a yellow colour of greater or lesser intensity; however, the UV/Vis absorption spectra differed significantly from salt to salt. Figure 2 shows, as an

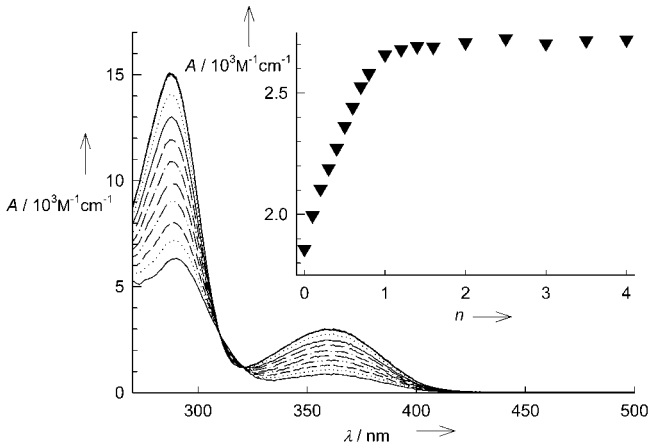

Figure 2. Spectrophotometric titration of a solution of $\mathbf{1}^+$ (4×10^{-5} M) in DMSO with a standard solution of tetrabutylammonium acetate in DMSO. Inset: molar absorbance at 360 nm versus number of equivalents of acetate (n) for a 5×10^{-6} M solution of $\mathbf{1}^+$.

example, the family of spectra obtained during the titration of $\mathbf{1}^+$ with acetate. The intensity of the bands at 290 and 360 nm (the latter being responsible for the yellow colour) progressively increased, reaching a limiting value of the molar absorbance (15700 and 3100 $M^{-1}cm^{-1}$, respectively) after the addition of one equivalent of acetate.

The titration profile shows a steep curvature, which should correspond to a particularly high equilibrium constant; however, the p parameter, (p = [concentration of complex]/[maximum possible concentration of complex]) was greater than 0.8, which prevents the reliable determination of an equilibrium constant.[6] Therefore, we can only state that log$K$ is greater than 6. Notably, even in the case of a more dilute solution (e.g., 5×10^{-6} M, as shown in the inset of Figure 2), a steep curvature was obtained and p was greater than 0.8.

Similar results were obtained following the titration of $\mathbf{1}^+$ with F^- and $H_2PO_4^-$; the bands at 290 and 360 nm increased in intensity and the same limiting values of the molar absorbances were reached (15700 and 3100 $M^{-1}cm^{-1}$, respectively, see also Table 1). In all cases, a 1:1 reaction stoichiometry was apparent; however, the steep curvature of the titration

Table 1. The equilibrium constants (logarithmic values) determined by the spectrophotometric titration of $\mathbf{1}^+$ (=LH^+) with anions X^-, and the molar absorbances ($M^{-1}cm^{-1}$) at 290 and 360 nm of the solutions containing $\mathbf{1}^+$ and excess of the anion in DMSO.

equilibrium: $LH^+ + X^- \rightleftharpoons L + HX$			
Anion	log$K$	ε_{290}	ε_{360}
CH_3COO^-	>6	15700	3100
F^-	>6	15700	3100
$H_2PO_4^-$	>6	15700	3100
equilibrium: $[LH]^+ + X^- \rightleftharpoons [LH\cdots X]^-$			
Anion	log$K$	ε_{290}	ε_{360}
Cl^-	4.52±0.02	4500	450
Br^-	3.55±0.02	3100	310
NO_3^-	2.97±0.04	3500	350

profile prevented determination of the equilibrium constant ($\log K > 6$).

Different results were obtained following titration of $\mathbf{1}^+$ with NO_3^-, Cl^- and Br^-. Although the intensity of absorption at 290 and 360 nm increased, the limiting values obtained after addition of excess anion were distinctly lower than those in the above examples, and varied according to the nature of the anion (see Table 1). As an example, Figure 3 displays the family of spectra obtained from the titration with Cl^-. In all cases, nonlinear least-squares analysis of the titration data indicated a 1:1 stoichiometry. In addition, the titration profiles displayed gentle curvature and the p parameter was less than 0.8.

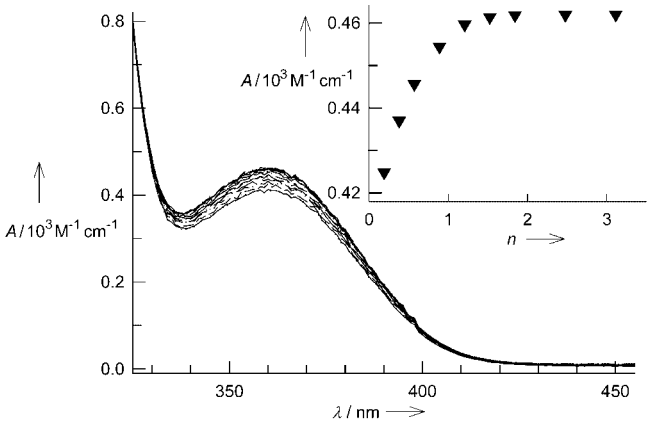

Figure 3. Spectrophotometric titration of a solution of $\mathbf{1}^+$ (9×10^{-4} M) in DMSO with a standard solution of benzyltributylammonium chloride in DMSO. Inset: molar absorbance at 360 nm versus number of equivalents of chloride (n).

The equilibrium constants, calculated from the nonlinear fitting of titration profiles, are reported in Table 1. The $\log K$ values for the $\mathbf{1}^+/X^-$ interaction decrease along the series: CH_3COO^-, F^-, $H_2PO_4^-$ > Cl^- > Br^- > NO_3^-.

Further insights into the nature of receptor–anion interactions were provided by the analysis of ^{1}H NMR spectra. Figure 4 displays the spectra for titration of a 10^{-2} M [D_6]DMSO solution of **1**-PF_6 with a [D_6]DMSO solution of [Bu_4N]CH_3COO. Upon addition of acetate, the -NH signal at $\delta = 11.6$ ppm disappears and the majority of signals pertinent to the -CH hydrogens shift distinctly upfield, with the greatest shift observed for -C(3)-H (Δppm = −0.64). Similar results were obtained for F^- and $H_2PO_4^-$, in particular, the same limiting δ values (obtained after the addition of one or more equivalents of anion) were recorded.

A different behaviour was observed with the remaining anions. Figure 5 shows the spectra obtained in the course of titration of $\mathbf{1}^+$ with benzyltributylammonium chloride in [D_6]DMSO. In contrast to the results for CH_3COO^-, F^- and $H_2PO_4^-$, the peak relative to the amide group (peak 1), did not disappear, but instead was shifted significantly downfield. The protons in positions 2, 3 and 5 were shifted downfield, whereas those in positions 4 and 6 remained unchanged. Similar results, although with less pronounced shifts, were observed upon titration with bromide.

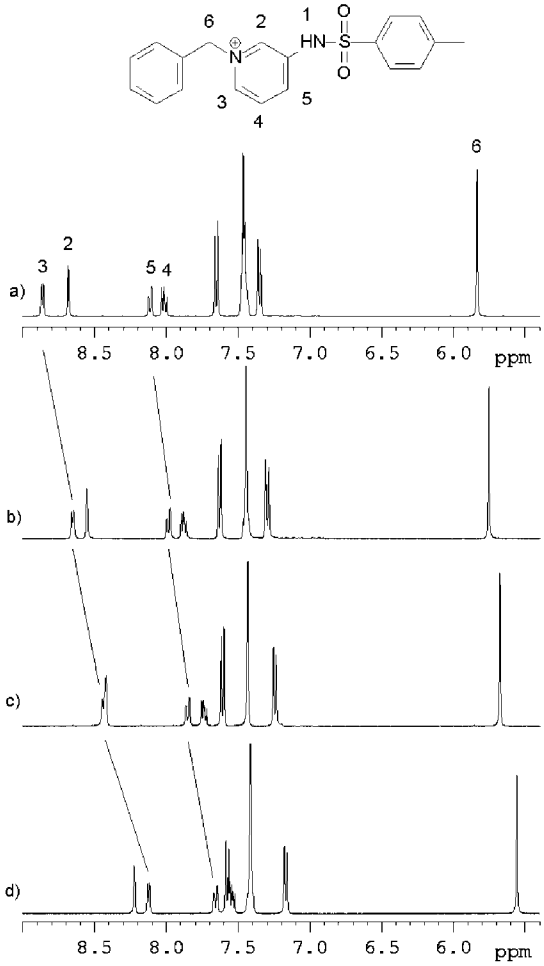

Figure 4. ^{1}H NMR titration of $\mathbf{1}^+$ in [D_6]DMSO (10^{-2} M) with a standard solution of tetrabutylammonium acetate in [D_6]DMSO. The spectra were recorded after the addition of a) 0, b) 0.25, c) 0.5 and d) 1.0 equivalents of acetate.

The slow evaporation of a water/acetonitrile (2:1 v/v) solution containing equimolar amounts of **1**-PF_6 and [Bu_4N]CH_3COO yielded pale yellow crystals. X-ray diffraction revealed that these crystals contained no anions; rather, the positive charge of the benzyl pyridinium group was balanced by the negative charge resulting from deprotonation of the -NH fragment of the amide subunit. The zwitterion is shown in Figure 6. Comparison with $\mathbf{1}^+$ revealed significant changes in the geometry of the sulfonamide group (Table 2).

Following deprotonation, the N(1)–S(1) bond length decreases, whereas the S=O distance increases. This suggests that the lone pair on the deprotonated nitrogen atom is partly delocalised by a π mechanism over the $>SO_2$ fragment. This is described in part by the resonance representation in Scheme 1 (formula **b**). On the other hand, some electronic charge must also delocalise through a π mechanism over the pyridinium ring, as suggested by the distinct reduction of the N(1)–C(1) distance and accounted for by the res-

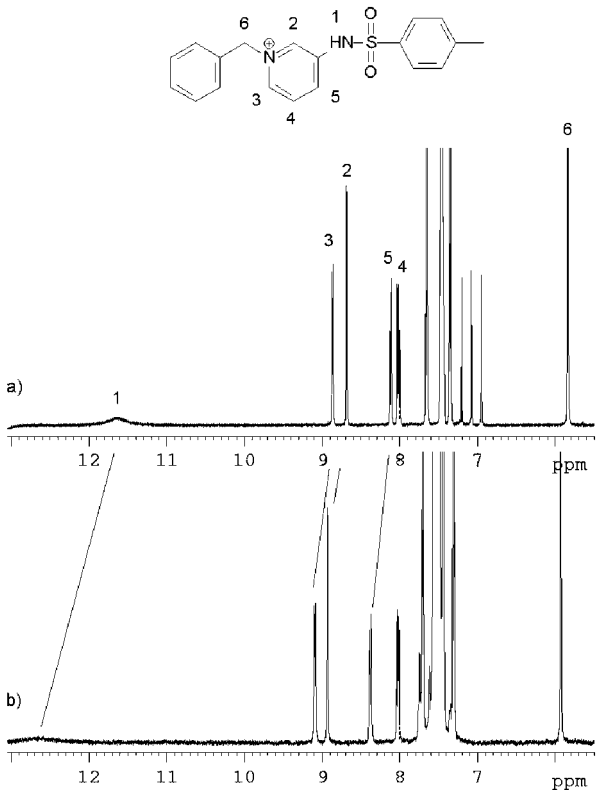

Figure 5. ^{1}H NMR titration of $\mathbf{1}^+$ in [D_6]DMSO (10^{-2} M) with a standard solution of benzyltributylammonium chloride in [D_6]DMSO. The spectra were recorded after the addition of a) 0 and b) 10 equivalents of the anion solution.

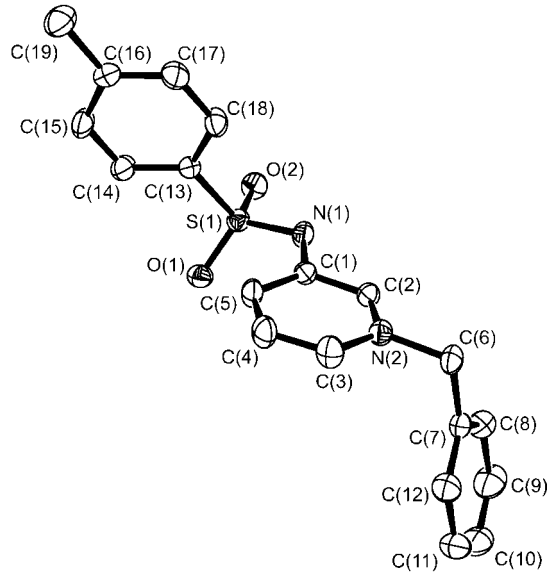

Figure 6. An ORTEP plot of the zwitterion $\mathbf{1}^+$ (thermal ellipsoids are drawn at the 30% probability level, hydrogens bonded to carbon atoms were omitted for clarity). The deprotonation of the N(1) atom ensures the electroneutrality of the molecule.

onance formula **c** in Scheme 1 (which is one of the several possible). The geometrical features of the sulfonamide group of the zwitterion are very similar to those of an analogous zwitterion, in which a methylpyridinium fragment is linked to a methylsulfonamide group (N–C: 1.372 Å; N–S: 1.581 Å; S=O: 1.455 and 1.448 Å; S–C: 1.765 Å).[7] Most interestingly, a DMSO solution of the zwitterionic compound showed the same spectroscopic features (UV/Vis and NMR spectroscopy) as a solution containing the **1**-PF_6 salt and a slight excess of [Bu_4N]X (in which $X^- = F^-$, CH_3COO^- or $H_2PO_4^-$). This unequivocally demonstrates that, on addition of F^-, CH_3COO^- or $H_2PO_4^-$ to a solution of **1**-PF_6, a proton is neatly transferred from $\mathbf{1}^+$ to X^-. In other words, a neutralisation process takes place between the acid $\mathbf{1}^+$ (or BH^+) and the base X^- (or A^-), according to the classical Brønsted proton transfer equilibrium (1).

Table 2. Selected bond lengths [Å] and angles [°] for the sulfonamide group in **1**-PF_6 and zwitterion **1**.

	1-PF_6	zwitterion **1**
N(1)–C(1)	1.411(3)	1.374(5)
N(1)–S(1)	1.644(3)	1.570(3)
S(1)–O(1)	1.439(2)	1.451(3)
S(1)–O(2)	1.419(2)	1.451(3)
S(1)–C(13)	1.748(3)	1.779(3)
C(1)-N(1)-S(1)	124.36(20)	120.51(26)
N(1)-S(1)-O(1)	103.14(13)	113.78(16)
N(1)-S(1)-O(2)	107.57(14)	106.39(16)
N(1)-S(1)-C(13)	106.24(14)	109.38(18)
O(1)-S(1)-O(2)	120.51(14)	114.84(16)
O(1)-S(1)-C(13)	109.46(14)	105.79(15)
O(2)-S(1)-C(13)	108.92(14)	106.36(16)

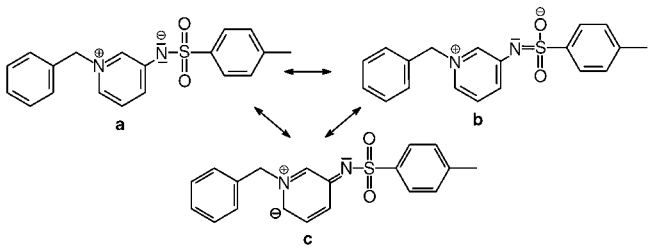

Scheme 1. Resonance representation of the deprotonated form of receptor $\mathbf{1}^+$. Formula **b** accounts for the shortening of the N–S bond and for the lengthening of the S=O bonds. Formula **c** accounts for the shortening of the N–C bond.

$$BH^+ + A^- \rightleftharpoons B + HA \quad (1)$$

The zwitterionic nature of **1** accounts for the spectroscopic properties observed: The deprotonation of -NH causes the formation of an electrical dipole with an especially large moment, which explains the hyperchromic effect observed in the absorption spectrum. Partial π delocalisation of the negative electrical charge over the entire molecular framework of the zwitterion accounts for an increase in the shielding effect and the consequential general upfield shift of -CH signals.

On the other hand, it is suggested that for Cl^-, Br^- and NO_3^- ions, a genuine hydrogen-bond interaction is established with the receptor $\mathbf{1}^+$. The occurrence of such an interac-

tion removes charge density from the receptor, which generates a general deshielding of protons. This effect is especially detectable for the amide proton, which is directly involved in the interaction, and for C(6)–H, C(2)–H and C(3)–H, which are adjacent to the positively charged pyridinium nitrogen atom. The downfield shift is less pronounced for Br^-, which, in view of the smaller electronegativity of bromine, competes to a lesser extent for the -NH proton, thus inducing a smaller deshielding effect.

The sequence of log$K$ values ($Cl^- > Br^- > NO_3^-$) reflects the decreasing intensity of the anion–receptor hydrogen-bond interaction. Notably, the different hydrogen-bond interaction energies correspond to the different molar absorbances of the UV/Vis bands, even if ε values do not correlate closely to log$K$ values.

On the basis of this evidence, the following empirical criterion for discerning neat proton transfer and true hydrogen-bond formation, following the interaction between an -NH-containing receptor and an anion, is tentatively proposed: a) A general upfield shift of proton signals within the NMR spectrum, together with high and constant limiting absorbance of UV/Vis bands, indicate deprotonation; b) a selective downfield shift and lower and variable ε values indicate authentic hydrogen-bond formation.

Next, we attempted to explain why receptor $\mathbf{1}^+$ transfers a proton to some anions (e.g., CH_3COO^-), but establishes hydrogen-bond interactions with others (e.g., Cl^-). The equilibrium constant (K) for the acid–base neutralisation equilibrium (1) results from the ratio of the two acidity constants (K_{BH+}/K_{HA}), and the pK_{HA} values for some organic and inorganic anions are known (e.g., pK_{HA} for CH_3COO^- is 12.3[8]). Therefore, having established that log$K$ for CH_3COO^- is >6, the pK_{BH+} value for $\mathbf{1}^+$ is calculated to be <6.3. In Figure 7, pK_a(HA/A$^-$) values for the anions investigated are tentatively positioned on the vertical scale on the right (CH_3COO^- and F^- have been set at the same level, even though acetate is slightly more basic). On the vertical scale on the left, the pK_a value of $\mathbf{1}^+$ is indicated. The two vertical lines are juxtaposed in such a way that the pK_a of $\mathbf{1}^+$ lies somewhere between the pK_{HA} of $H_2PO_4^-$ and the pK_{HA} of Cl^-. For anions whose pK_{HA} values are higher than the pK_{BH+} of $\mathbf{1}^+$, the equilibrium constant for the acid–base neutralisation equilibrium (1) is distinctly higher than 1 and proton transfer occurs. On the other hand, for anions whose pK_a values are lower than the pK_a of $\mathbf{1}^+$, the neutralisation equilibrium is not favoured and the hydrogen-bond interaction is not followed by definitive proton transfer. Therefore, the occurrence of a Brønsted acid–base equilibrium or the establishment of a hydrogen-bond interaction in a given medium depends simply on the acidity of the receptor's -NH group with respect to the basicity of the anion. Anions whose pK_{HA} value is lower than the pK_a of the -NH acid (i.e., below the solid horizontal line in Figure 7) will establish a true hydrogen-bond interaction, whereas anions with higher pK_a values (above the dashed line) will induce definitive -NH deprotonation and the formation of HA.

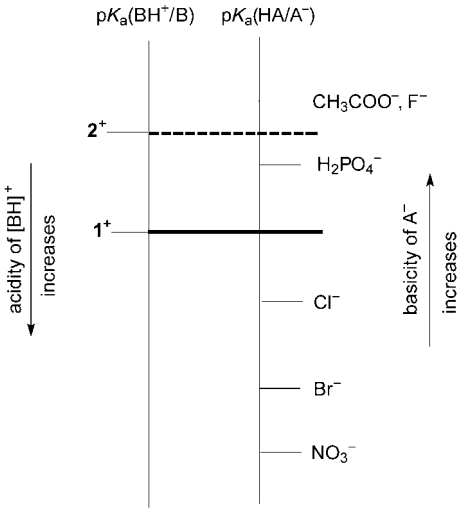

Figure 7. Matching of the acidity scale for the receptor $[BH]^+$ and the basicity scale for A^- (pK_a values for anions are tentative; CH_3COO^- and F^- have been arbitrarily assigned the same pK_a value). Receptor $\mathbf{1}^+$ transfers a proton to anions that lie above the solid horizontal line and establishes a true hydrogen-bond interaction with the anions that lie below the line. Receptor $\mathbf{2}^+$ transfers a proton to anions that lie above the dashed horizontal line and establishes a true hydrogen-bond interaction with the $H_2PO_4^-$ ion, which remains below the dashed horizontal line. Cl^- and anions that lie below this line exhibit a basicity that is too low and a hydrogen-bond-acceptor tendency that is too poor to enable them to interact with $\mathbf{2}^+$.

We tested the reliability of this approach by considering a further -NH-containing receptor $\mathbf{2}^+$. This possesses a pyrrole-type -NH fragment, whose intrinsic acidity is lower than that of sulfonamide, and should be enhanced by the presence of a proximate pyridinium group. In this receptor, the -NH fragment is separated from the $>N^{\oplus}$ group by two benzene carbon atoms, as in $\mathbf{1}^+$.

Figure 8 displays the family of spectra obtained when a solution of **2**-PF_6 in DMSO (8.4×10^{-4} M) was titrated with a

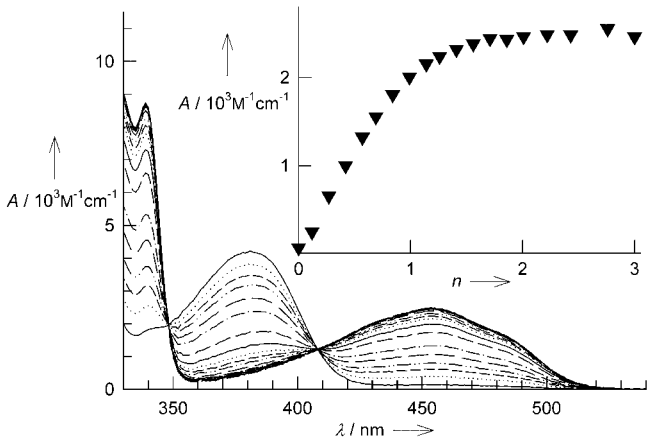

Figure 8. Spectrophotometric titration of a solution of $\mathbf{2}^+$ in DMSO (8.4×10^{-4} M) with a standard solution of tetrabutylammonium acetate in DMSO. Inset: molar absorbance at 454 nm versus the number of equivalents of acetate (n) for a 1×10^{-4} M solution of $\mathbf{2}^+$.

standard solution of $[Bu_4N]CH_3COO$. Upon acetate addition, the absorption band at 380 nm decreases, whereas a new band at 454 nm develops and increases in intensity to a plateau after the addition of one equivalent of anion (the titration profile in the inset of Figure 8 refers to a solution of 1×10^{-4} M). The smooth curvature of the titration profile enables the accurate determination of the equilibrium constant (see Table 3).

Table 3. The equilibrium constants (logarithmic values) determined by the spectrophotometric titration of $\mathbf{2}^+$ ($=LH^+$) with anions X^-, and the molar absorbances ($M^{-1}\,cm^{-1}$) at 454 nm of the solutions containing $\mathbf{2}^+$ and excess of the anion in DMSO.

equilibrium: $LH^+ + X^- \rightleftharpoons L + HX$		
Anion	log$K$	ε_{454}
CH_3COO^-	5.10 ± 0.05	2300
F^-	4.77 ± 0.02	2300
equilibrium: $[LH]^+ + X^- \rightleftharpoons [LH\cdots X]^-$		
Anion	log$K$	ε_{454}
$H_2PO_4^-$	3.11 ± 0.01	1800

Figure 9 shows the ^{1}H NMR spectra obtained during the titration of a $[D_6]$DMSO solution of $\mathbf{2}^+$ with $[Bu_4N]CH_3COO$. All of the -CH signals are shifted upfield; the most significant shifts are for the carbolinium unit, due to the decreasing positive charge on the pyridinium fragment (maximum Δppm $=-0.4$ for -C(5)–H and -C(6)–H). Similar results for limiting absorbance and δ of -CH signals (upfield shift) were obtained upon titration with fluoride. The log$K$ value, calculated from the titration profile, is 4.77 ± 0.02. These results indicate neutralisation and proton transfer, following the interaction of $\mathbf{2}^+$ with acetate and fluoride. In addition, using the relationship $K=K_{BH+}/K_{HA}$ and the reported pK_{HA} value for CH_3COO^- in DMSO, the pK_{BH+} for $\mathbf{2}^+$ is calculated to be 7.2. Therefore, the higher acidity of sulfonamide with respect to pyrrole is maintained in the presence of a proximate, positively charged group. Deprotonation of a pyrrole subunit in the presence of F^- in a CH_2Cl_2 solution has been recently observed.[9]

Figure 10 shows the family of UV/Vis spectra obtained upon titration of a solution of $\mathbf{2}^+$ in DMSO with $[Bu_4N]H_2PO_4$ (titration profile in the inset, calculated log$K=3.11\pm0.01$). The limiting value of the molar absorbance at 454 nm is notably lower than that observed upon titration with CH_3COO^- and F^- (see Table 3).

Figure 11 displays the ^{1}H NMR spectra obtained during the titration of a solution of $\mathbf{2}^+$ in DMSO with $[Bu_4N]H_2PO_4$. There is a significant downfield shift of the proton in position 5 (Δppm $=+0.27$); in addition, the upfield shifts of the other carbolinium protons are less intense than those observed in the titration with acetate. No shift is observed for the aliphatic group -CH_2-, which is bound directly to the positively charged nitrogen atom. On the basis of this, we suggest that a true hydrogen-bond interaction is established between $\mathbf{2}^+$ and $H_2PO_4^-$, and that -C(5)–H is directly involved in this interaction. Notably, addition of the

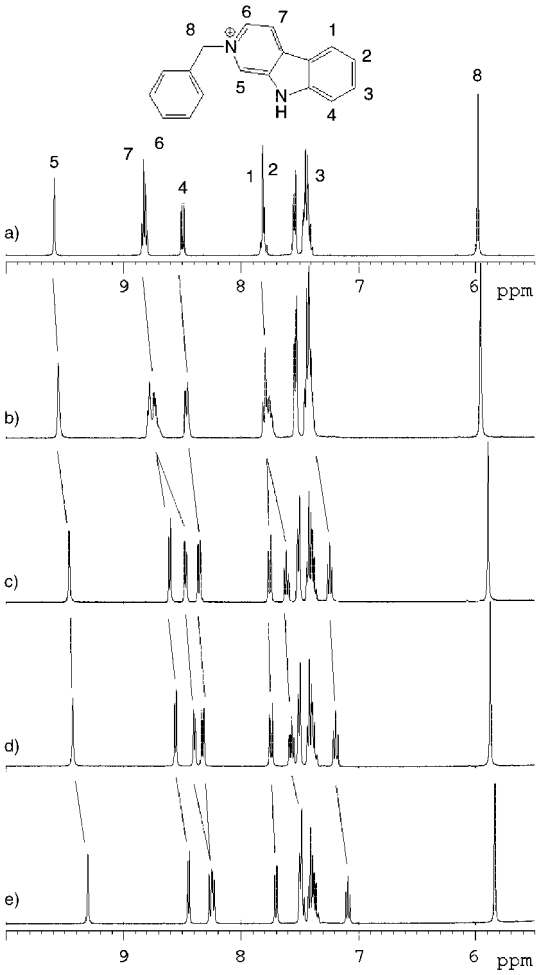

Figure 9. ^{1}H NMR spectra for the titration of $\mathbf{2}^+$ in $[D_6]$DMSO (10^{-2} M) with a standard solution of tetrabutylammonium acetate in $[D_6]$DMSO. The spectra were recorded after the addition of a) 0, b) 0.25, c) 0.75, d) 1.0 and e) 2.0 equivalents of acetate.

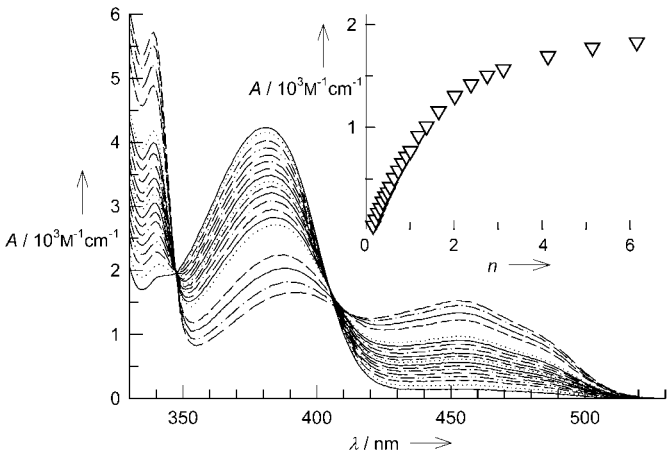

Figure 10. Spectrophotometric titration of a solution of $\mathbf{2}^+$ in DMSO (8.2×10^{-4} M) with a standard solution of tetrabutylammonium monobasic phosphate in the same solvent. Inset: the molar absorbance at 454 nm versus the number of equivalents of phosphate (n).

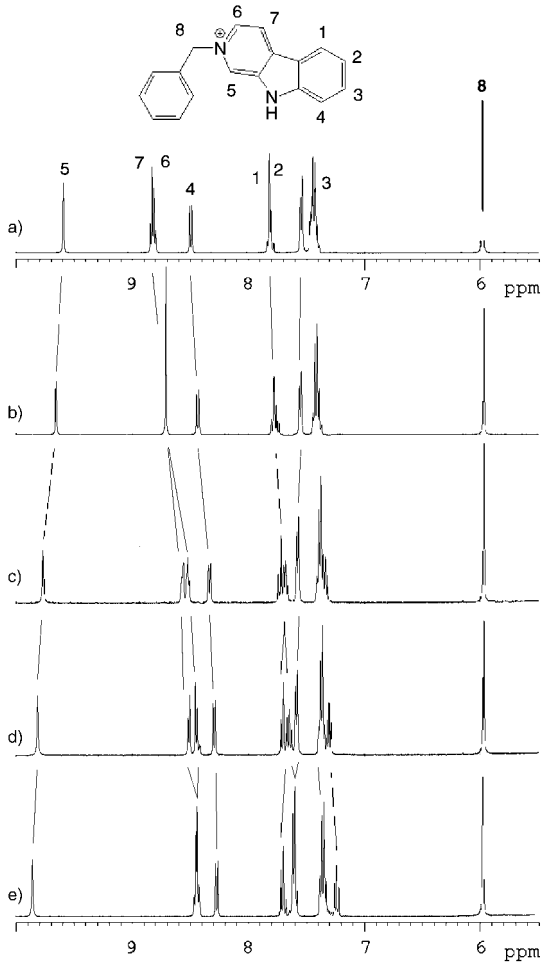

Figure 11. ^{1}H NMR spectra for the titration of $\mathbf{2}^+$ in [D$_6$]DMSO (10^{-2} M) with a standard solution of tetrabutylammonium monobasic phosphate in [D$_6$]DMSO. The spectra were recorded after the addition of a) 0, b) 0.25, c) 0.75, d) 1.0 and e) 2.0 equivalents of phosphate.

butylammonium salts of other anions (NO_3^- and halides) caused no significant modification of the UV/Vis and ^{1}H NMR spectra, indicating a lack of interaction. Therefore, the less acidic receptor $\mathbf{2}^+$ can still transfer a proton to the moderately strong bases CH_3COO^- and F^-, establish hydrogen-bond interactions with $H_2PO_4^-$, and does not interact at all with the weakly basic anions Cl^-, Br^- and NO_3^-. This scenario is represented in Figure 7. The pK_{BH+} of $\mathbf{2}^+$ must now be positioned between the pK_{HA} values of CH_3COO^-, F^- and $H_2PO_4^-$, thus distinguishing between acid–base neutralisation (above the dashed horizontal line) and hydrogen-bond formation (below). Cl^- and other anions exhibit a basicity that is too low and a hydrogen-bond-acceptor tendency that is too poor to enable them to interact with $\mathbf{2}^+$.

Conclusion

Figure 7 is generally applicable for the solvent used in this study (DMSO); however, a qualitatively similar diagram would be expected for an analogous solvent, for example, MeCN. Although most of the significant anions are represented on the right-hand vertical line, a number of -NH receptors of varying acidity have yet to be placed and correctly juxtaposed on the left-hand vertical line. This diagram should be helpful in the design of anion receptors. For example, to increase the hydrogen-bond-donor tendency of the receptor, particularly acidic -NH groups could be chosen, or acidity could be enhanced by using electron-withdrawing substituents (e.g., $-NO_2$, $-CF_3$, -CN). However, high receptor acidity may induce neat proton transfer, which is beyond the realm of supramolecular chemistry and within the domain of classical Brønsted acid–base reactions. Ideally, the pK_a of the -NH-containing receptor should be coincident with (or slightly more positive than) the pK_{HA} of the A^- anion, corresponding to the premise that the strongest hydrogen-bond interactions are established between an anion A^- and its conjugate acid HA (which indeed refer to the same pK_a value).[10]

Experimental Section

4-Methyl-*N*-pyridin-3-yl-benzensulfonamide: A solution containing 3-aminopyridine (1.5 g, 15.9 mmol) in pyridine (70 mL) and 4-methylbenzenesulfonyl chloride (3.8 g, 19.9 mmol) was refluxed for 2 h, then the reaction mixture was poured onto iced water (150 mL). The white precipitate was collected by filtration under vacuum and washed with pure water (yield 3.35 g; 85%). The product purity was controlled by performing TLC (SiO_2, 100% AcOEt: $R_f = 0.5$). $C_{12}H_{12}N_2SO_2$ (248 g mol^{-1}). ^{1}H NMR (400 MHz, [D$_6$]DMSO): $\delta = 10.50$ (s, 1H; NH), 8.28 (d, 1H; C*H* py), 8.25 (d, 1H; C*H* py), 7.63 (d, 2H; C*H* bz), 7.50 (dd, 1H; C*H* py), 7.36 (d, 2H; C*H* bz), 7.28 (dd, 1H; C*H* py), 2.4 ppm (s, 3H; CH_3).

1-Benzyl-3-(toluene-4-sulfonylamino)pyridinium hexafluorophosphate (1-PF$_6$): An amount of 4-methyl-*N*-pyridin-3-yl-benzensulfonamide (0.4 g, 1.6 mmol) was dissolved in $CHCl_3$ (70 mL). An excess of benzyl bromide (0.41 g, 2.4 mmol) was added and the resulting solution was refluxed for 24 h. The solvent was then removed by using a rotary evaporator to give an oily residue, which was dissolved in hot water and treated with a saturated aqueous solution of NH_4PF_6. The white precipitate of **1**-PF_6 was recovered by filtration under vacuum (yield 0.45 g; 83%). $C_{19}H_{17}N_2SO_2PF_6$ (484 g mol^{-1}). ^{1}H NMR (400 MHz, [D$_6$]DMSO): $\delta = 11.65$ (s, 1H; NH), 8.86 (d, 1H; CH(7)), 8.68 (s, 1H; CH(4)), 8.11 (d, 1H; CH(5)), 8.01 (dd, 1H; CH(6)), 7.65 (d, 2H; CH(2)), 7.46 (m, 5H; bz), 7.34 (d, 2H; CH(1)), (d, 2H; CH(2)), 5.84 (s, 2H; CH_2(8)), 2.4 ppm (s, 3H; CH_3).

2-Benzyl-9*H*-β-carbolin-2-ium (2-PF$_6$): An amount of β-carboline (0.11 g, 0.65 mmol) was dissolved in $CHCl_3$ (70 mL). An excess of benzyl bromide (0.16 g, 0.98 mmol) was added and the resulting solution was refluxed for 24 h. The solvent was then removed by using a rotary evaporator to give a yellow solid residue, which was dissolved in hot water and treated with a saturated, aqueous solution of NH_4PF_6. The white precipitate of **1**-PF_6 was recovered by filtration under vacuum (yield 0.21 g; 80%). $C_{18}H_{15}N_2PF_6$ (404 g mol^{-1}). ^{1}H NMR (400 MHz, CD_3CN): $\delta = 9.1$ (s, 1H; CH(5)), 8.55 (d, 1H; CH(7)), 8.45 (s, 1H; CH(6)), 8.40 (d, 1H; CH(4)), 7.80 (dd, 2H; CH(1)-CH(2)), 7.50 (m, 6H; C*H*(3), bz), 5.85 ppm (s, 2H; CH_2(8)).

General procedures and materials: All reagents for syntheses were purchased from Aldrich/Fluka and used without further purification. UV/Vis spectra were recorded on a Varian CARY 100 spectrophotometer with a quartz cuvette (path length: 1 cm). NMR spectra were recorded on a Bruker Avance 400 spectrometer, operating at 9.37 T. Spectrophotometric titrations were performed at 25°C on 10^{-4} and 10^{-5} M solutions of **1**-PF_6 and **2**-PF_6 in DMSO (polarographic grade). Aliquots of a fresh

Bu_4NX standard solution were added and the UV/Vis spectra of the samples were recorded. Spectrophotometric titration curves were fitted by using the HYPERQUAD program.[11] ^1H NMR titrations were carried out in [D$_6$]DMSO at moderately high concentrations of **1**-PF_6 and **2**-PF_6 (10^{-2} M).

X-ray crystallographic studies: Diffraction data were collected at ambient temperature by using an Enraf–Nonius CAD4 four-circle diffractometer, working with graphite-monochromatised $Mo_{K\alpha}$ radiation ($\lambda = 0.71073$ Å). Crystal data for the **1**-PF_6 complex and for the $\mathbf{1}^+$ zwitterion are reported in Table 4. Data reductions (including intensity integration, background, Lorentz and polarisation corrections) were performed with the WinGX package.[12] Absorption effects were evaluated with the psi-scan method,[13] and absorption correction was applied to the data (min./max. transmission factors were 0.865/0.938 for **1**-PF_6 and 0.931/0.970 for **1**).

Table 4. Crystallographic data for **1**-PF_6 and zwitterion **1**.

	1-PF_6	zwitterion **1**
formula	$C_{19}H_{19}F_6N_2O_2PS$	$C_{19}H_{18}N_2O_2S$
M	484.40	338.42
colour	colourless	pale yellow
dimension [mm]	$0.80\times0.43\times0.21$	$0.80\times0.28\times0.11$
crystal system	triclinic	orthorhombic
space group	$P\bar{1}$ (no. 2)	$P2_1$ (no. 4)
a [Å]	6.1779 (8)	10.3645(16)
b [Å]	12.8573(17)	8.5655(12)
c [Å]	13.3607(18)	10.7356(14)
α [°]	83.866(12)	–
β [°]	87.840(16)	115.083(12)
γ [°]	82.756(22)	–
V [Å^3]	1046.5(2)	863.2(2)
Z	2	2
ρ_{calcd} [g cm^{-3}]	1.537	1.302
$\mu Mo_{K\alpha}$ [mm^{-1}]	0.303	0.201
scan type	ω-2θ scans	ω-2θ scans
θ range [°]	2–26	2–26
measured reflections	5213	2181
unique reflections	4104	2084
R_{int}[a]	0.0116	0.0213
strong data [$I_o > 2\sigma(I_o)$]	2673	1685
$R1$, $wR2$ (strong data)[b]	0.0492, 0.1136	0.0393, 0.0849
$R1$, $wR2$ (all data)[b]	0.0879, 0.1323	0.0594, 0.0941
GoF[c]	1.040	1.029
refined parameters	320	217
max./min. residuals [eÅ^{-3}]	0.22/−0.17	0.22/−0.17

[a] $R_{int} = \Sigma|F_o^2 - F_o^2(\text{mean})|/\Sigma F_o^2$. [b] $R1 = \Sigma||F_o| - |F_c||/\Sigma|F_o|$, $wR2 = \{\Sigma[w(F_o^2 - F_c^2)^2]/\Sigma[w(F_o^2)^2]\}^{1/2}$, in which $w = 1/[\sigma^2 F_o^2 + (aP)^2 + bP]$ and $P = [\max(F_o^2, 0) + 2F_c^2]/3$. [c] $GoF = \{\Sigma[w(F_o^2 - F_c^2)^2]/(n-p)\}^{1/2}$, in which n is the number of reflections and p is the total number of refined parameters.

Crystal structures were solved by direct methods (SIR 97),[14] and refined by full-matrix least-square procedures on F^2 using all reflections (SHELXL 97).[15] Anisotropic displacement parameters were refined for all non-hydrogen atoms. Hydrogens bonded to carbon atoms were placed at calculated positions with the appropriate AFIX instructions and refined by using a riding model; hydrogens bonded to the N(1) atom of **1**-PF_6 were located in the ΔF map and refined, constraining the N–H distance to be 0.89 ± 0.02 Å.

CCDC-237092 and CCDC-237093 contain the supplementary crystallographic data for this paper. These data can be obtained free of charge via www.ccdc.cam.ac.uk/conts/retrieving.html (or from the Cambridge Crystallographic Data Centre, 12 Union Road, Cambridge CB21EZ, UK; fax: (+44) 1223-336-033; or deposit@ccdc.cam.ac.uk).

Acknowledgement

We thank Dr. Laura Linati (Centro Grandi Strumenti, Università di Pavia) for the NMR characterisation of the samples and Dr. Enrico Monzani (Dipartimento di Chimica Generale, Università di Pavia) for assistance with the NMR titrations and helpful discussions. The financial support of the European Union (RTN Contract HPRN-CT-2000–00029) and of the Italian Ministry of University and Research (PRIN, Dispositivi Supramolecolari; FIRB, Project RBNE019H9K) is gratefully acknowledged.

[1] P. A. Gale, *Coord. Chem. Rev.* **2003**, *240*, 1.
[2] C. Suksai, T. Tuntulani, *Chem. Soc. Rev.* **2003**, *32*, 192.
[3] R. Martinez-Mañez, F. Sancenón, *Chem. Rev.* **2003**, *103*, 4419.
[4] R. J. Fitzmaurice, G. M. Kyne, D. Douheret, J. D. Kilburn, *J. Chem. Soc. Perkin Trans. 1* **2002**, 841.
[5] K. Choi and A. D. Hamilton, *Coord. Chem. Rev.* **2003**, *240*, 101.
[6] C. S. Wilcox in *Frontiers in Supramolecular Chemistry and Photochemistry*, Wiley-VCH, Weinheim, **1991**, pp. 123–143.
[7] N. Dennis, A. R. Katritzky, H. Wilde, E. Gavuzzo, A. Vaciago, *J. Chem. Soc. Perkin Trans. 2* **1977**, 1304.
[8] F. Bordwell, *Acc. Chem. Res.* **1988**, *21*, 456.
[9] S. Camiolo, P. A. Gale, M. B. Hursthouse, M. E. Light, A. I. Shi, *Chem. Commun.* **2002**, 758.
[10] T. Steiner, *Angew. Chem.* **2002**, *114*, 50; *Angew. Chem. Int. Ed.* **2002**, *41*, 48.
[11] P. Gans, A. Sabatini, A. Vacca, *Talanta* **1996**, *43*, 1739.
[12] L. J. Farrugia, *J. Appl. Crystallogr.* **1999**, *32*, 837.
[13] A. C. T. North, D. C. Phillips, F. S. Mathews, *Acta. Crystallogr. Sect. A* **1968**, *24*, 351.
[14] A. Altomare, M. C. Burla, M. Camalli, G. L. Cascarano, C. Giacovazzo, A. Guagliardi, A. G. G. Moliterni, G. Polidori, R. Spagna, *J. Appl. Crystallogr.* **1999**, *32*, 115.
[15] G. M. Sheldrick, SHELX97 Programs for Crystal Structure Analysis, University of Göttingen, Germany, **1997**.

Received: June 10, 2004
Published online: November 10, 2004

